Ground Reaction Curve to Analyze Segmental Lining in Tunneling

S. Chaiyaput, T.N. Huynh and M. Sugimoto
Department of Civil and Environmental Engineering, Nagaoka University of Technology, Japan

ABSTRACT: Both of conventional tunnelling and shield tunnelling methods can be applied to Diluvial and Neogene deposits, on which megacities are located in Japan. Since the lining design methods for both tunnelling methods are very different, a unified concept for tunnel lining design is expected. Therefore, a frame structure analysis model for tunnel lining design using the ground reaction curve had been developed, which can take into account the excavated surface displacement to active state and the overcutting effect. In this paper, to discuss its performance, the measured earth pressure on the lining at a site in Diluvial deposit was compared with the calculated one by the developed model and the conventional model. As a result, it was confirmed that the developed model can represent the earth pressure on the lining reasonably.

1 INTRODUCTION

The deep underground in Japan are mainly composed of Diluvial and Neogene deposits, in which both of conventional tunnelling and shield tunneling methods can be applied. However, both lining design methods are very different, so a unified concept for tunnel lining design is expected. For this reason, a few guidelines for both of urban conventional tunnelling and shield tunnelling were issued such as Japan Society of Civil Engineering (1996) and (2003) in Japan, and ERTC9 (1997) in Europe.

Based on the above mentioned background, the unified tunnel lining design method had been developed by applying the nonlinear ground reaction curve by Sugimoto and Sramoon (2002) in frame structure analysis. To present the performance of the developed model, a site study was carried out, and the measured earth pressure on the lining at the site was compared with the calculated one by the developed and conventional models.

2 NUMERICAL MODELING

2.1 *Analysis model*

The numerical model is constructed for two segment rings based on the beam spring model by Murakami and Koizumi (1978) and the ground reaction curve by Sugimoto and Sramoon (2002), as shown in Fig. 1. In the model, segmental joints, ring joints, and surrounding ground are considered and represented by rotation springs, shear springs, and ground springs, respectively. In addition, backfill grouting is examined through various grouting rates.

2.2 *Surrounding ground*

Surrounding ground applies earth pressure on tunnel lining. To involve initial earth pressure and effects of ground displacement, the surrounding ground is modeled by ground springs, which have the relationship between the coefficient of earth pressure in vertical and horizontal directions, K_v and K_h, and the distance from the initial excavation surface to the lining, u_n(+: outward), as shown in Fig. 2. Fig. 2 shows the ground reaction curve with the conventional model by JSCE (2006).

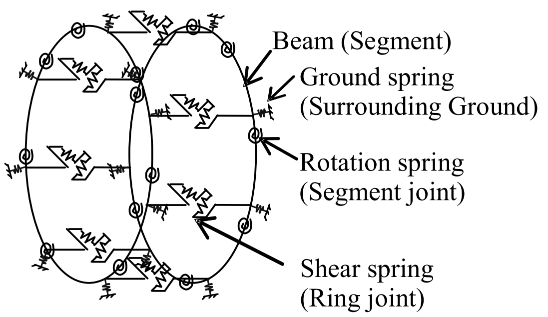

Fig. 1. Analysis model

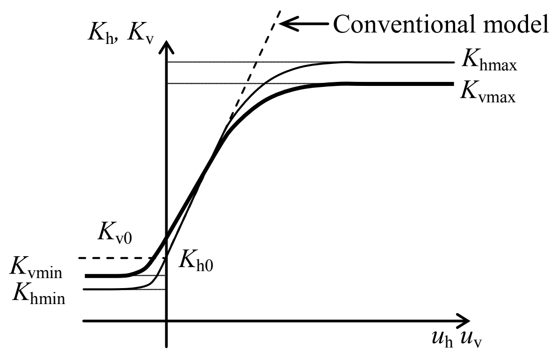

Fig. 2. Ground reaction curve

The ground reaction curve can be represented by

$$K_h(u_n) = \begin{cases} (K_{h0} - K_{h\min})\tanh\left(\dfrac{a_h u_n}{K_{h0} - K_{h\min}}\right) + K_{h0} & (u_n \le 0) \\ (K_{h0} - K_{h\max})\tanh\left(\dfrac{a_h u_n}{K_{h0} - K_{h\max}}\right) + K_{h0} & (u_n \ge 0) \end{cases} \tag{1}$$

$$K_v(u_n) = \begin{cases} (K_{v0} - K_{v\min})\tanh\left(\dfrac{a_v u_n}{K_{v0} - K_{v\min}}\right) + K_{v0} & (u_n \le 0) \\ (K_{v0} - K_{v\max})\tanh\left(\dfrac{a_v u_n}{K_{v0} - K_{v\max}}\right) + K_{v0} & (u_n \ge 0) \end{cases} \tag{2}$$

where K_{h0} = coefficient of earth pressure at rest; K_{v0} = coefficient of initial vertical earth pressure normally equal to 1; subscripts max and min indicate the upper and lower limits of the coefficient of earth pressure, respectively; a_h and a_v = gradient of function K_h and K_v at u_n = 0, respectively. Moreover, the coefficient of earth pressure in any direction, K_θ, can be interpolated as

$$K_n(u_n,\theta) = K_v(u_n)\cos^2\theta + K_h(u_n)\sin^2\theta \tag{3}$$

where θ = angle measured from downward vertical direction to u_n.

The ground spring is connected to the lining at one end and fixed at the outer end in the model. The initial earth pressure σ_{n0} is applied as pre-stressed load throughout the ground spring. During the analysis, corresponding to the ground reaction curve, the change of earth pressure $\triangle\sigma_n$ will be generated. As a result, the total earth pressure on the lining σ_n is calculated as below

$$\begin{aligned} \sigma_n &= \sigma_{n0} + \Delta\sigma_n \\ \sigma_{n0} &= K_n(0,\theta)\sigma_{v0} \\ \Delta\sigma_n &= (K_n(u_n,\theta) - K_n(0,\theta))\sigma_{v0} \end{aligned} \tag{4}$$

2.3 *Backfill grouting*

Due to overcutting, the earth pressure on the lining is usually less than the earth pressure at rest. Moreover, backfill grouting is usually applied to overcutting of segmental tunnels. It directly influences on the displacement of the excavation surface as well as the resultant earth pressure. Therefore, it is necessary to consider earth pressure involving grouting effects. To represent overcutting length, tail void t_v was adopted. To consider the effect of backfill grouting, effective grouting

Table 1. Site data

Item	Component	Value
Ground	Overburden depth (GL-m)	22.208
	Groundwater level (GL-m)	11.175
	Overbuden ratio	2.725
TBM	Type	Slurry shield
	Outer diameter (m)	8.310
Segment	Type	RC
	Outer diameter (m)	8.150
	Width (m)	1.200
	Thicknnes (m)	0.375
	Number of segment joint	8
	Number of ring joint	29
Grouting	Timing	Immediate
	Tail void (m)	0.080
	Grouting pressure ave. (kPa)	500
	Grouting pressure max. (kPa)	600
	Grouting rate	No records

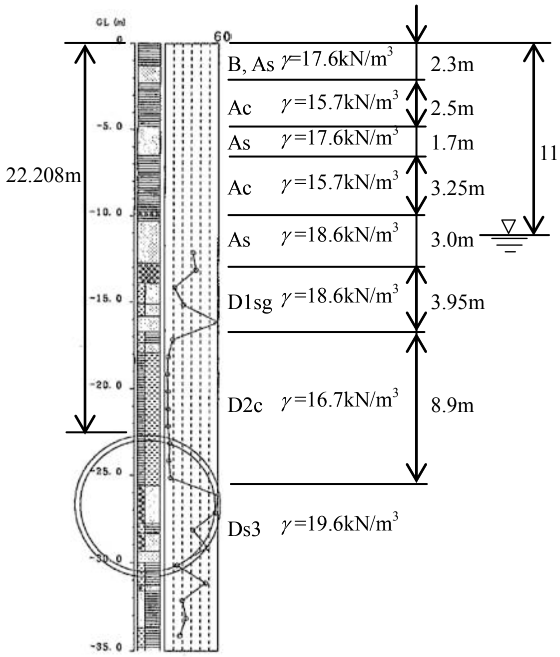

Fig. 3. Geological profile

rate α_g was adopted. Then, the actual gap between the tunnel lining and the excavation surface after backfill grouting, which is named initial excavation surface displacement, u_{init}, can be represented as

$$u_{init} = t_v(\alpha_g - 1) \tag{5}$$

In order to consider the backfill grouting, enforced displacement was applied to the outer end of the ground spring to generate pressure of backfill grouting acting on the lining. The enforced displacement is equivalent to the initial gap and determined in Eq. (5).

Table 2. Analysis conditions

Item	Component	Value
Ground	Effective earth p. at crown (kPa)	342.27
	Water p. at crown (kPa)	300.80
	Coef. of earth p. K_{hmin}, K_{h0}, K_{hmax}	0.0, 0.5, 5.0
	K_{vmin}, K_{v0}, K_{vmax}	0.0, 1.0, 5.0
	Coef. of subground reaction k_h, k_v (MN/m^3)	9.8, 9.8
	Tangential ground spring const. k_t (MN/m^3)	0.001
Segment	Young's modulus (GN/m^2)	33
	Poison's ratio	0.2
	Unit weight (kN/m^3)	28
	Radius of centroid (m)	3.935
	Rotation spring const. at segment joint (MN-m/rad)	42.5
	Noramal spring const. at ring joint (MN/m)	478
	Tangential spring const. at ring joint (MN/m)	1050
Design	Vertical earth pressure	Overburden load
	Ground water treatment	Effective earth pressure method

3 APPLICATIONS

3.1 *Analysis conditions*

The model has been applied for simulations of a tunnel constructed in Osaka, Japan. The tunnel of 8.15m in outer diameter was constructed in Diluvial sand at 22.2m deep. The groundwater level is GL-11.2m. The ground properties and site data are shown in Table 1 and Fig. 3.

In the analysis, the effective grouting rate α_g and the coefficient of subgrade reaction k_n are taken as parameters, since these properties give much effect on the effective earth pressure on the lining σ_n' and their values are uncertain. Other analysis conditions are shown in Table 2.

3.2 *Influence of coefficient of subgrade reaction and effective grouting rate on earth pressure acting on segments*

To grasp the influence of the effective grouting rate α_g and the coefficient of subgrade reaction k_n on the effective earth pressure on the lining σ_n', the parametric study has been carried out for a range of α_g from 80% to 110% and a range of k_n from 10MN/m^3 to 1000 MN/m^3. Fig. 4 shows the calculated σ_n' at crown, spring line (SL), and invert with the σ_n' measured by a pad type earth pressure gauge, which is introduced by Kojima et al. (2002). From this figure, the followings are found:

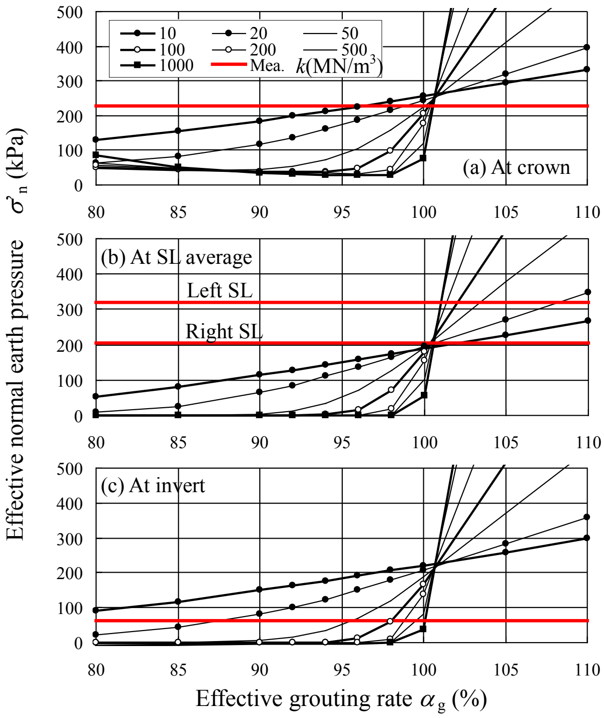

Fig. 4. Influence of coefficient of subground reaction k and effective grouting rate α_g on effective normal earth pressure σ'_n

1) When α_g is less than a certain value, σ_n' is close to 0. Except for the above, as α_g increases, σ_n' increases gradually up to α_g = 100%, but in case of α_g > 100%, σ_n' increases greatly;
2) As k_n increases, σ_n' becomes close to 0 in case of α_g < 100%, and σ_n' increases greatly in case of α_g > 100%; and
3) σ_n' at crown is slightly larger than σ_n' at invert. σ_n' at spring line is less than σ_n' at crown and invert, but, it is larger than the lateral earth pressure ratio times σ_n' at crown and invert.

These can be considered as follows:
1) α_g defines the gap between ground and initial excavation area u_{init} in Eq. (5). That is, α_g < 100%, α_g > 100% means the active state, passive state in Fig. 2, respectively. Since u_{init} defines σ_n' through Eqs. (1) – (4), the influence of α_g on σ_n' appears;
2) k_n defines the slope of ground reaction curve in Fig. 2. Therefore, as k_n increases, the change of σ_n' increases around α_g = 100%;
3) In this analysis, since the effective stress method is adopted as ground water treatment shown in Table 2, and the buoyancy is larger than the self-weight of segments, the buoyancy lifts up the segments, then σ_n' at crown is larger than σ_n' at invert; and
4) In this analysis, since the lateral earth pressure ratio is 0.5, and the σ_n' is redistributed due to the stiffness of the segments, the σ_n' distribution appears.

Based on the above examinations, the range of α_g and k_n, for which the measured σ'_n and the calculated σ'_n match, is shown in Table 3. From the view point that the α_g is expected to be close to 100%, the k_n is supposed to be around 200MN/m^3.

3.3 *Comparison with the measured data*

Fig. 5 shows the total earth pressure σ_n distribution along the segment surface under α_g = 100% and k_n = 200MN/m^3 calculated by the proposed model and the conventional model with the theoretical and measured total earth pressure σ_n and the hydraulic pressure σ_w. From this figure, the followings are found:

1) The shape of the measured σ_n distribution is flattened horizontally. The measured σ_n at crown is close to the initial total earth pressure σ_{n0}, that at spring line is a little bit larger than the σ_{n0}, and that at invert is less than the σ_{n0};

2) The shape of the σ_n distribution calculated by the proposed model is more circle than that of the theoretical σ_{n0}. Its difference from the measured σ_n is less than 70kPa at most except for left spring line; and

3) The σ_n calculated by the conventional model around crown and spring line is larger than the measured σ_n and that at invert is close to the σ_{n0}. The σ_n calculated by the conventional model is larger than the measured σ_n by 80 to 260 kPa except for left spring line. This indicates that the calculated sectional force of the lining is excess, compared with the actual one.

These can be considered as follows:

1) Since the grouting pressure is about equal to the overburden load, and the measured σ_n is close to the σ_{n0}, α_g is considered to be about 100%;

2) The equilibrium conditions of the segment in horizontal and vertical directions are not satisfied, based on the measured σ_n. This is considered that the measured σ_n on each ring has fluctuation due to wriggle motion of the TBM, even the summation of the σ_n on each ring along tunnel axis direction satisfies the equilibrium condition. Taking account of the above, the calculated σ_n by the proposed model could represent the measured σ_n to a certain degree; and

3) The conventional model can not represent the measured σ_n. This is because the conventional model does not take account of passive state in Fig. 2, and initial excavation surface displacement u_{init}.

4 CONCLUSIONS

In this study, the proposed frame structure model with the ground reaction curve was applied to the site data, and the measured earth pressure on the lining at the site was compared with the calculated one by the developed model and the conventional model. Based on the results, it is concluded that the proposed model produces the effective earth pressure on the lining reasonably, compared to other model.

Table 3. k and α_g corresponding to measured σ'_n

Position	Coefficient of ground reaction k (MN/m^3)		
	50	100	200
Crown, SL	101	101	101
Invert	96	98	99

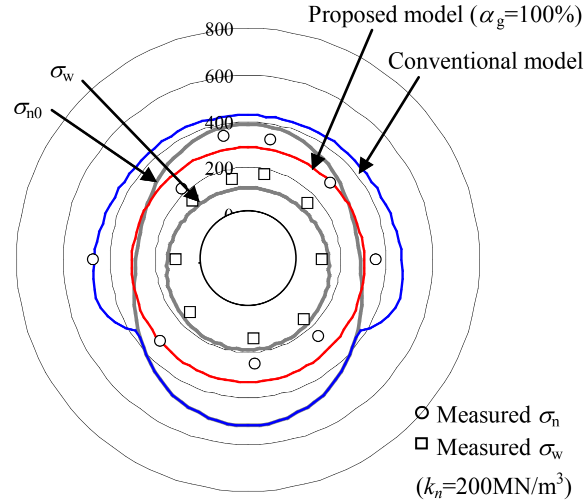

Fig. 5. Comparison of earth pressure on tunnel lining, σ_n (kPa) interpreted in different models

REFERENCES

ERTC9, (1997). *Recommendations of the ERTC9 - Bored Tunnels*, Ernst & Sohn, Berlin, Germany.

Japan Society of Civil Engineering. (1996). *The Boundary Region Between the Urban NATM and the Shield Tunneling - Future Direction and Current Procedure of Structural Design*, JSCE, Tokyo, Japan (in Japanese).

Japan Society of Civil Engineering. (2003). *The Boundary Region Between the Urban NATM and the Shield Tunneling - The State of the Art on Evaluation of Load*, JSCE, Tokyo, Japan (in Japanese).

Japan Society of Civil Engineering. (2006). *Standard Specifications for Tunneling - 2006, Shield Tunnels*, JSCE, Tokyo, Japan.

Kojima, S., Hashimoto, T., and Nagaya J. (2002). "In-site measurement on earth pressure acting on segment of underground river tunnel." *Proc. of Tunnel Engineering, Japan Society of Civil Engineering*, 12, 501-506.(in Japanese)

Murakami, H., Koizumi, A. (1978). "Study on load bearing capacity and mechanics of shield segment ring." *J. of Japan Society of Civil Engineering*, 272, 103-115.(in Japanese)

Sugimoto, M., Sramoon, A. (2002). "Theoretical model of shield behavior during excavation. I: Theory." *J. of Geotechnical and Geoenvironmental Engineering*, 128(2), 138-155.